

CLUSTER 3: Imaging Electrons at the Nanoscale

Coordinator: Raymond Ashoori

Raymond Ashoori (Physics, MIT)	Charles M. Marcus (Physics, Harvard)
Bertrand I. Halperin (Physics, Harvard)	Venky Narayanamurti (SEAS & Physics, Harvard)
Eric Heller (Chemistry&Physics, Harvard)	Michael Stopa (NNIN, Harvard)
Jennifer Hoffman (Physics, Harvard)	Robert Westervelt (SEAS & Physics, Harvard)
Marc Kastner (Physics, MIT)	Amir Yacoby (Physics, Harvard)

Collaborators: M. Manfra, L. Pfeiffer, K.W. West (Lucent Technologies), R.D. Dupuis (Georgia Tech.)

International Collaborators: Fabio Beltram (NEST, Pisa, Italy), Leo Kouwenhoven (TU Delft, The Netherlands), Daniel Loss (University of Basel, Switzerland), Hiroyuki Sakaki (University of Tokyo, Japan), Lars Samuelson (Lund University, Sweden), and Seigo Tarucha (University of Tokyo and NTT, Japan)

Number of postdoctoral fellows: 2

Number of graduate students: 6

Number of undergraduate students: 3

Introduction

Electrons and photons inside nanoscale structures display striking behavior that arises from the confinement of quantum waves. By visualizing how electrons move through nanoscale systems, we can understand the fundamental science and develop new quantum devices. These devices can direct electron flow, or control the motion of electron charges and spins for nanoelectronics, spintronics, or quantum information processing.

Nanoscale structures are also promising for photonics: they can control the motion of optical waves using sub-wavelength devices. Near-field Scanning Optical Microscopy (NSOM) can be used to image and perturb these photonic systems.

The goal of the ***Imaging at the Nanoscale*** cluster is to develop new ways to image electrons and photons inside nanoscale systems, including their quantum behavior. This is difficult for electrons, because they are buried inside the structure, and because low temperatures are necessary. Nanoscale imaging of photonic systems also requires new approaches. This Cluster brings together a group of investigators who have designed and built scanning probe microscopes and developed new imaging techniques to image electrons and photons inside nanoscale systems. Close collaborations with theorists allow us to understand what the images mean. We have strong international collaborations with Fabio Beltram (NEST), Leo Kouwenhoven (Delft), Daniel Loss (Univ Basel), Hiroyuki Sakaki (Univ Tokyo), Lars Samuelson (Luft Univ) and Seigo Tarucha (Univ Tokyo & NTT).

Expected outcomes of this research are:

New Approaches to Imaging Electrons and Photons inside Nanoscale Systems — New imaging techniques use custom-made scanning probe microscopes and theoretical analysis to understand the quantum behavior of electrons and photons inside nanoscale

systems. These techniques are based on cooled Scanning Probe Microscopes (SPMs) capacitively coupled to the electrons below, Magnetic Force Microscopes (MFMs), Scanning Tunneling Microscopes (STMs), Ballistic Electron Emission Microscopy (BEEM), and Electron Emission Luminescence (EEL) Microscopy. Near-field Scanning Optical Microscopy (NSOM) using custom tips can be used to investigate photonic systems. The investigators are experts in the design and fabrication of scanning probe microscopes.

New Nanoelectronic and Photonic Devices — Visualizing and understanding the motion of electrons and photons will allow us to explore new types of nanoelectronic and photonic devices and systems based on nanocrystals and nanowires from the *Nanoscale Building Blocks* Cluster, and semiconductor heterostructures grown at the MBE Lab at UC Santa Barbara. These new materials offer exciting opportunities. Imaging, coupled with theoretical simulations, will allow us to understand how these new devices work.

Significant Achievements

In the past year, a number of custom-made scanning probe microscopes have been constructed by Center faculty:

Jennifer Hoffman has completed the construction of a cooled, magnetic force microscope. It is a custom design, with a laterally moving magnetic tip. High spatial resolution and sensitivity are provided by a silicon cantilever tip with a 20 nm radius, and by a carbon-nanotube based tip (in collaboration with Alex de Lozanne at the Univ. of Texas Austin).

Hoffman plans to use the instrument to image vortices in high T_c superconductors. She also plans to understand the role of impurities in quantum cascade lasers, in collaboration with Capasso, by imaging the surface potential of cleaved laser heterostructures. Multiferroics, materials that combine two of the following properties - ferromagnetic, ferroelectric, and ferroelastic - are also of interest.

Venky Narayanamurti has constructed a new dual-tip STM/BEEM instrument, which can be cooled to 100 K, and is located inside a UHV chamber. One tip can be used to inject electrons into a small nanocrystal, while the other tip acts as a gate, making this a very useful instrument for the characterization of the nano building blocks developed in Cluster 2 of our Center. He plans to measure tunnel-induced luminescence from CdSe nanocrystals in different dielectric environments.

Amir Yacoby has developed a cooled scanning probe microscope which has a single-electron-transistor (SET) charge sensor at the end of the tip. He has used this instrument to image density fluctuations in a graphene flake.

Graphene is an unusual material that consists of a single layer of carbon atoms. Its energy band structure is the same as a massless relativistic particle. Because there is no bandgap, an electron can easily change into a hole, and back to an electron. Disorder is thought to break up the carriers in an uncharged graphene flake into islands of electrons and holes. Using his SET-based microscope, Yacoby has observed this phenomenon.

Theorists Bertrand I. Halperin and Eric Heller have performed calculations and simulations that allow us to understand what happens in the imaging experiments.

Halperin has investigated the spatial behavior of a one-dimensional electron gas. These calculations are relevant to experiments by Yacoby on cleaved edge overgrowth samples, and to work by Westervelt on InAs nanowires grown by Samuelson. For low electron densities, the electron-electron correlations are stronger, and the electron gas enters the Wigner-crystal regime, with a periodic charge modulation and an antiferromagnetic ordering of spins. In an applied magnetic field, ferromagnetic ordering occurs. These findings address the fundamental behavior of electrons inside narrow channels, and they are of importance for future nanoelectronic devices.

Heller has simulated STM images of electron waves inside a hexagonal quantum corral formed by CO molecules on a (111) copper surface, for comparison with experimental images from Hari Manoharan's group at Stanford. He finds good agreement, both in zero and moderately strong applied magnetic fields, showing that the STM images truly represent quantum waves.

Physics of Graphene Sheets

Raymond Ashoori

Physics, Massachusetts Institute of Technology

Collaborators: B.I. Halperin, H. Park, A. Yacoby (Harvard University); Pierre Petroff (Univ. of Calif., Santa Barbara), Jak Chakhalian (Univ. of Arkansas); Loren Pfeiffer (Bell Labs/Alcatel-Lucent Technologies)

Andre Geim's lab at the University of Manchester in the UK recently announced a fantastic discovery. They found that by simply rubbing graphite on surfaces (and later applying ultrasound to the surfaces to flake off excess graphite) they can deposit isolated monolayers of graphite (graphene sheets). Extraordinarily, they found it was easy to make electrical contacts and to fashion Hall bars from the material. At low temperatures, the graphene sheets actually display the quantum Hall effect! This effect has been reproduced in Philip Kim's lab. at Columbia, and they have found mobilities as high as $15,000 \text{ cm}^2/\text{Vs}$. The physics of the QHE in these structures is quite different from other 2-D systems. Other than the valley degeneracy, the band structure has a linear rather than parabolic dispersion relation, and although Landau level structure exists (the levels are no longer evenly spaced in energy), the derivation involves solving a Dirac equation. Another feature of the material is that it can easily be field-effect-doped with a back gate with electrons or holes.

Obviously, this new technology is very interesting for a number of technological reasons. Carbon appears to have an amazing immunity to developing surface traps that drastically lower the mobility of most field effect devices. Indeed, it took many years to develop CMOS transistors, and the main difficulty was overcoming the threshold broadening induced by surface states. Carbon nanotubes transistors, on the other hand, simply worked, essentially on the first try. The carbon nanotubes have also displayed very high current carrying capacities and high transconductances. It is likely that the graphene sheets will display the same characteristics.

An obvious experiment for us is to perform our charge accumulation imaging on the graphene sheets. As the tip can, in this case be moved up directly against the surface, we can expect much higher resolution. Moreover, we will be able to perform direct STM imaging along with our capacitance techniques. We note though that capacitance has an important feature lacking in STM. In STM, the bias set between the tip and the sample controls the tunneling current and cannot be adjusted independently of the tunneling current. Therefore, even at small biases one often ends up with large electric fields between the tip and the sample due to workfunction differences. In capacitance, there is no tunneling current, and we can adjust (and null) at will the electric field between the tip and sample and thereby control the perturbation created by the tip. Finally, having the tip so close to the sample will allow for very high resolution scanned gate measurements.

We plan to perform the same types of scanning bubble experiments on graphene in the quantum Hall effect regime as we have done in GaAs. This will give us a good idea of the types of short-range disorder that exist in these structures. Later experiments may examine high current saturation in the material (as occurs in nanotubes) and conducting pathways. This is perhaps the most exciting new electronic materials systems to arise in

the last decade. Knowledge both of the underlying physics and techniques for producing graphene gained in this project will have impact on the NSEC further in the future. This work will impact on our understanding of nanotubes and 2-D systems and connect with the work of [Park](#) and also [Halperin](#). The work is also closely related to that of [Yacoby](#) – it will complement [Yacoby](#)'s work

We have learned to make graphene sheets using Geim's technique, and we can easily make electrical contact to these sheets. One major difficulty in our scanning imaging experiments is finding the small piece of graphene (typically ~10 microns in size) in the scan range of our microscope. The initial coarse approach of our microscope tip may result in the tip landing a few mm away from the graphene piece. Our microscope has a 15 micron field of view. So, finding the graphene piece requires coarse lateral walking. We needed to develop a method, utilizing only tip-to-sample capacitance images to find the graphene piece.

Our method consists of coating the sample surface in metal (so that we have a capacitance signal) with holes in the metal in the shape of marks. These marks tell us how to walk with our microscope towards the graphene piece. We have recently succeeded in imaging these marks, and we can now walk to the graphene piece. We hope that in the next several months, we will be able to perform our capacitance imaging on graphene at low temperatures (300 mK).

Figure 3.1. (*right*) Pattern of marks for guiding our tip to the location of a graphene piece. (*below*) Image of a mark taken with our capacitance microscope.



Along with this work, we are also working on a new kind of spectroscopy of quantum Hall systems (with partial NSEC support). This is described in the “Highlights” section.

Physics of Scanning-Probe Microscope Imaging of Nanoscale Systems

Eric Heller

Chemistry, Physics, Harvard University

Collaborators: Carol Lynn Alpert (Museum of Science, Boston), Don Eigler (IBM Almaden), Hari Manoharan (Stanford), R.M. Westervelt (Harvard)

International Collaborator: Tobias Kramer (University Regensburg, Germany)

Research Goal, Approach and Accomplishments. Our goals have included understanding the physics of SPM tip imaging in semiconductor microstructures, and using that knowledge to understand the physics of the electron flow itself. In addition, we have undertaken a study of spin precession, and its effects on imaging, in these same microstructures.

Imaging Electrons in Nanowires

The Heller group has embarked on an ambitious program to understand and predict the imaging of strongly correlated electrons in quantum wires, including tip potentials and self-consistent electric fields, etc. This involves the detailed solution of a quantum few body problem, for 4 or 5 electrons, including full correlation, spin-charge entanglement, and accurate wave functions and one particle densities. These calculations are somewhat taxing, requiring as they do rather large matrices, which need to be diagonalized. So far, the algorithm is in place to find the eigenfunctions in the absence of the imaging tip potential, and calculations are underway for including the tip. We expect interesting phenomena to crop up, including the effects of charge density waves, and charges squeezing across the tip potential. Certainly there will also be some surprises.

SPM Imaging

The Heller group is a theoretical group with long experience in scattering theory and an array of numerical and theoretical tools at our disposal, many of which we developed ourselves. We have previously shown why SPM tip imaging can yield sharp images including quantum fringes, and last year we extended that work to include the new physics of transconductance imaging in a magnetic field, in a study of magnetic focusing. Complex images which at first looked like they might contain no clear message or physics were revealed instead to be pregnant with information regarding electrons buffeted by magnetic fields, walls, and random spatially fluctuating potentials.

The SPM imaging theory continues with a new student and new challenges, including understanding of the QPC physics in the tunneling (almost pinched-off) regime, where the QPC enters a new regime and starts to act like an STM point source with interference between outgoing and backscattered amplitude (which does not happen for one or more transverse modes open in the QPC).

STM Imaging of Quantum Corrals in a Magnetic Field

The Heller group has started another line of research with the Manoharan group at Stanford, in a effort (which looks like it will be successful) to understand quantum corral STM images in strong magnetic fields, and additionally to come to some understanding

the pseudo-boundary conditions which walls of surface adatoms impose on surface state electrons, i.e., those electrons which are responsible for the interference structures seen in the corral experiments. The magnetic field imaging is being addressed by a Green's function technique. Many details and questions are coming up as fast as we can handle them and this looks like a very fruitful area for research, which promises to tell us much more about the nature of electronic processes on surfaces.

New Approach to the Quantum Hall Effect

The Heller group, together with former postdoc Tobias Kramer, has a new and somewhat controversial approach to the "ordinary" Quantum Hall effect and some extraordinary experiments, which we have also explained. It has long been known that electrons are injected at a singular point at one corner in a Hall bar, and they leave by a diagonally opposite point. These regions have singular potentials and have been seen experimentally as "hot spots" where almost all of the dissipation occurs. What has not been appreciated is that by adopting a "point source" time-dependent Green's function at the singular injection region, the conductance plateaus not only emerge naturally, but moreover explain some new fractional conductance effects (not the fractions in Laughlin's theory, rather other small fractions) seen experimentally under conditions of higher electric field. This view is extremely natural when viewed from the perspective of the STM imaging and quantum point contact conductance plateaus, which put the physics exactly at the tunneling region and the autocorrelation of a Green's function. But from the current QHE picture our view is diametrically opposed, in that we do not even require information on the fate of the electrons once they leave the corners, except that they sound not return. This we find in our preliminary simulations, which include donor atom potential random fluctuations in the effective field.

High Spatial Resolution Magnetic and Electrostatic Force Microscope

Jennifer Hoffman

Physics, Harvard University

Collaborators: Federico Capasso (Harvard University); Alex de Lozanne (University of Texas, Austin)

Research Goal, Approach, and Accomplishments: The goal of this project is to detect and measure both magnetic and electrostatic forces with 10 nanometer spatial resolution and sub-picoNewton force resolution. This imaging technology has many potential uses. Some initial systems we plan to study include:

1. Vortices in high temperature superconductors, via magnetic force microscopy.
2. Impurities in the junctions of the quantum cascade lasers under development in Capasso's laboratory, via Kelvin force microscopy.
3. Multi-ferroics, via both magnetic force microscopy and Kelvin force microscopy.

Superconducting Vortices

Superconductors have many potential uses, including:

- macroscopic generation of large magnetic fields, for medical diagnostics or basic scientific research.
- microscopic SQUIDS, for sensitive magnetic field detection in medicine, materials quality control, and many other applications.

These applications are presently limited by the uncontrolled dissipative motion of vortices (magnetic flux quanta). Although much research has been devoted to understanding average vortex properties, little is known about the microscopic motion and pinning of single vortices.

On the other hand, controlled vortex motion presents new opportunities for computing. Collectively controlled vortex motion can serve as a rectifier [1], a vortex ratchet mechanism can perform clocked logic [2], and vortices can control spins in an adjacent diluted magnetic semiconductor [3].

Given these challenges and opportunities, it is imperative to gain a better understanding of single vortex pinning. We have constructed a magnetic force microscope with vertical geometry to directly access the dominant lateral vortex pinning forces.

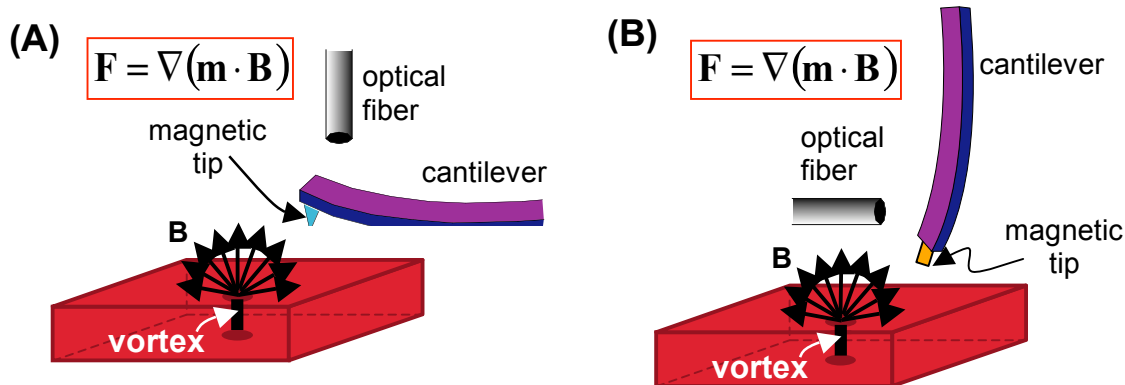


Figure 3.2. (A) Standard magnetic force microscope geometry: horizontal cantilever detects vertical force gradients. (B) New magnetic force microscope geometry: vertical cantilever detects horizontal force gradients. This geometry is more suitable for studying the pinning of vortices in superconductors.

Quantum Cascade Lasers

Professor Federico Capasso's group is working to increase the power output in mid-IR quantum cascade lasers (QCL). They believe that laser power output may be limited by imperfections in the junctions between $\text{Al}_{1-x}\text{In}_x\text{As}$ and $\text{Ga}_{1-x}\text{In}_x\text{As}$ layers, and resultant inhomogeneous charge accumulation. However, they have no means to image the local electronic structure of the boundary regions.

We plan to use our new force microscope in Kelvin force probe mode to image the surface potential of a cleaved QCL heterostructure. The cantilever is driven via capacitive coupling as an AC voltage at the cantilever resonance is applied to the sample. The driving force is minimized when the local DC voltage difference between tip and sample is minimized; therefore we use the measured cantilever oscillation amplitude as an error signal to feed back on the applied tip-sample DC voltage, as we scan. This enables a local measure of surface potential, and therefore a map of imperfections in the boundary regions.

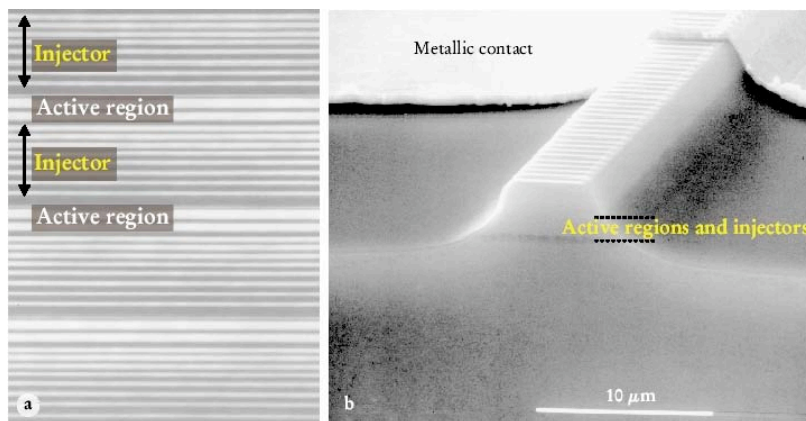


Figure 3.3. Figure taken from Capasso et al., *Physics Today* article, May 2002, p. 35. (A) TEM image of $\text{Al}_{0.6}\text{In}_{0.4}\text{As}$ and $\text{Ga}_{0.38}\text{In}_{0.62}\text{As}$ heterostructure. TEM cannot resolve the electrostatic potential due to imperfections at the boundaries between these layers. (B) Quantum cascade laser in the standard rectangular mesa waveguide configuration.

Multi-ferroics

A “multi-ferroic” material is one which has at least two of the following orders simultaneously: ferromagnetic, ferroelectric, and ferroelastic. The most famous example is the magnetoelectric effect, in which one can tune the electrical polarization by an external magnetic field. Until recently, this effect has always been very small – barely observable and certainly not technologically relevant. But the recent discovery of gigantic magnetoelectric effect in TbMnO_3 has revitalized this field. In TbMnO_3 , the electrical polarization can be switched from c -axis to a -axis by magnetic field. In addition to the fundamental physics questions raised by this anomalously large magnetoelectric effect, there are potentially significant implications for data storage.

Our microscope will be ideally suited to study this new class of multi-ferroic materials, as we have the capability to measure both the magnetic and the electrical parts of this effect.

Instrument Design and Construction

Graduate student Sang Chu designed the MFM, fridge, and vacuum system. Undergraduate Hasan Korre assembled components of the coarse motion system for 3-axis tip-sample positioning: He built electronic hardware and wrote software both to control and detect motion. Undergraduate Max Chalfin assembled and tested the mechanical components of the low temperature stepper motors for use in aligning the fiber optic detection system. Graduate student Tess Williams has created a process to use the focused ion beam to fabricate vertical cantilever tips with high aspect ratio and radius of curvature. The project is now led by postdoc Dr. Jeehoon Kim, who has tested and wired the cryostat, and assembled all components of the MFM system. Using the new microscope, Jeehoon has recently obtained the first proof-of-principle images of a magnetic floppy disk and magnetic hard drive.

The force microscope is now poised for high resolution imaging of magnetic and electrostatic signatures in novel materials, from newly discovered correlated electron materials, to newly fabricated man-made devices. Perhaps even more importantly, the microscope may be used not only for passive imaging, but also for active manipulation of the material or device being studied. The nanoscale magnet on the end of the cantilever may be used to drag vortices between pinning sites, to flip nanoscale bits, or to manipulate spins in diluted magnetic semiconductors.

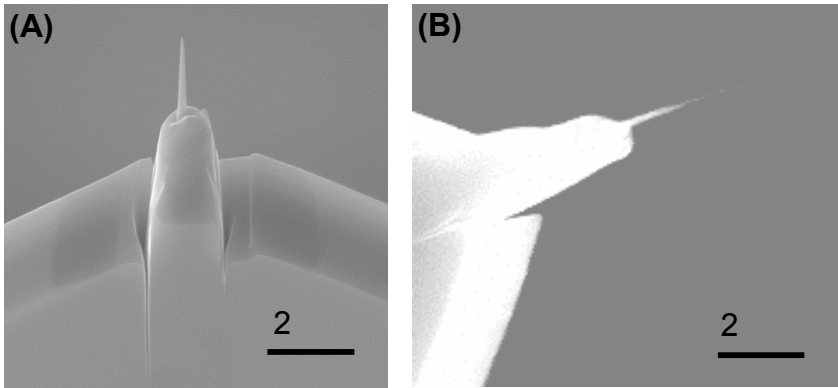


Figure 3.4. (A) Silicon cantilever tip with 20 nm radius, fabricated using the focused ion beam (FIB) in the Center for Nanoscale Systems (CNS). (B) Carbon nanotube tip fabricated by Dr. Jeehoon Kim in collaboration with Prof. Alex de Lozanne at University of Texas, Austin.

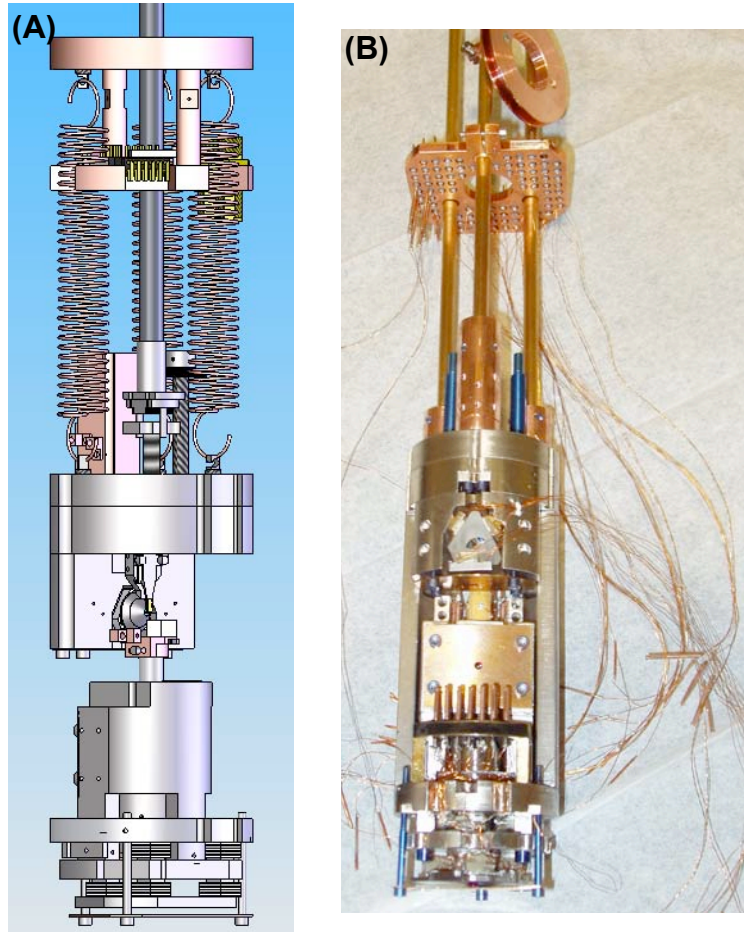


Figure 3.5. (A) The magnetic force microscope design has been completed, and the parts machined by the Harvard shop in the Engineering Sciences Laboratory. The drawing shows the instrument layout. (B) The photo shows the titanium (non-magnetic) body of the microscope containing the assembled z-axis coarse motion system, and x-y translation plates beneath: the triangular sapphire (low friction) beam will hold the fiber optic moving towards the cantilever.

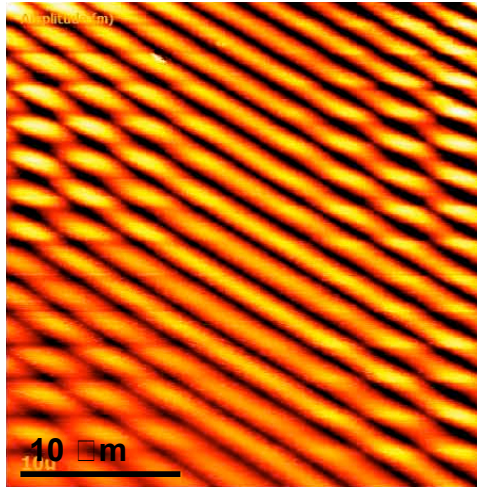


Figure 3.6. First image of a magnetic hard drive, acquired with a FIB-etched silicon cantilever tip, coated with 20 nm Co and 20 nm Cr. The image was acquired in ambient conditions.

References

- [1] J. E. Villegas *et al.*, *Science* **302**, 1188 (2003).
- [2] M. B. Hastings *et al.*, *Phys. Rev. Lett.* **90**, 247004 (2003).
- [3] M. Berciu, T. G. Rappoport, B. Jankó, *Nature* **435**, 71 (2005).

Control of a Double Quantum Dot in an InAs/InP Nanowire by an SPM Tip

Robert M. Westervelt

SEAS and Physics, Harvard University

Collaborators: Donhee Ham (SEAS, Harvard), Eric Heller (Chemistry and Physics, Harvard)

International Collaborators: Daniel Loss (University of Basel), Lars Samuelson (Lund University), and Seigo Tarucha (University of Tokyo)

Research Goal, Approach and Accomplishments

The goal of this research is to develop ways to individually tune the charge of tunnel coupled nanowire double dots, by using the conducting tip of a cooled scanning probe microscope (SPM) as a movable gate. Using chemical beam epitaxy, Samuelson's group can grow very small InAs quantum dots defined by InP barriers; an example is shown in Figure 3.7. The dots are shaped like hockey pucks, and tunneling occurs along the flat faces. These quantum dots have the advantages that they can be very small (~ 50 nm diameter by ~ 20 nm thickness), increasing the energy spacing of electron quantum states, permitting operation at higher temperatures, and that the g -factor for electrons is large, easing the manipulation of spins for spintronic applications. However they can be difficult to control using conventional lithographically fabricated side gates, because their size is comparable or smaller than the spatial resolution of e-beam lithography.

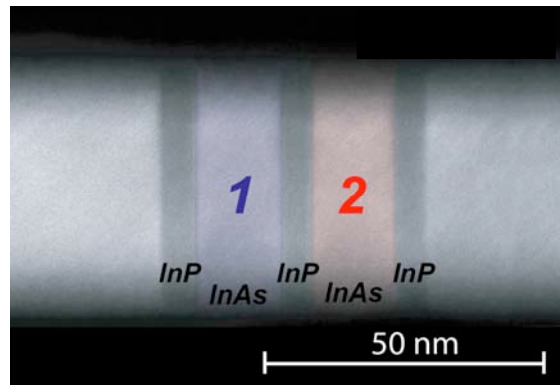


Figure 3.7. TEM image of a tunnel-coupled InAs double dot with InP barriers, grown in an InAs/InP nanowire heterostructure. Optimized growth technique leads to dots of nearly identical size. (Samuelson)

We plan to control nanowire double dots by using the tip of a cooled SPM as a movable gate, as illustrated by the simulations in Figure 3.8. A device is made by attaching source and drain leads to a nanowire that lies sideways on a substrate; the SPM tip is scanned in a plane slightly above. The number of electrons on a dot is controlled by the charge $C_{td}V_{tip}$ induced by the tip where the tip-to-dot capacitance C_{td} and V_{tip} is the tip voltage. By varying the tip-to-dot distance, the numbers of electrons m and n on the two dots can be individually controlled, using the bulls eye shaped charging diagrams shown on the left in Figure 3.8.

Planned experiments will measure the conductance image for the double dot, shown on the right in Figure 3.8. For the series double dot, conductance can only occur when both dots are on a Coulomb blockade conductance peak, at the boundary between m and $m + 1$ electrons in the charging diagram, shown at left. So the simulated image of double dot conductance vs. tip position, shown on the right, has peaks where the bulls eye

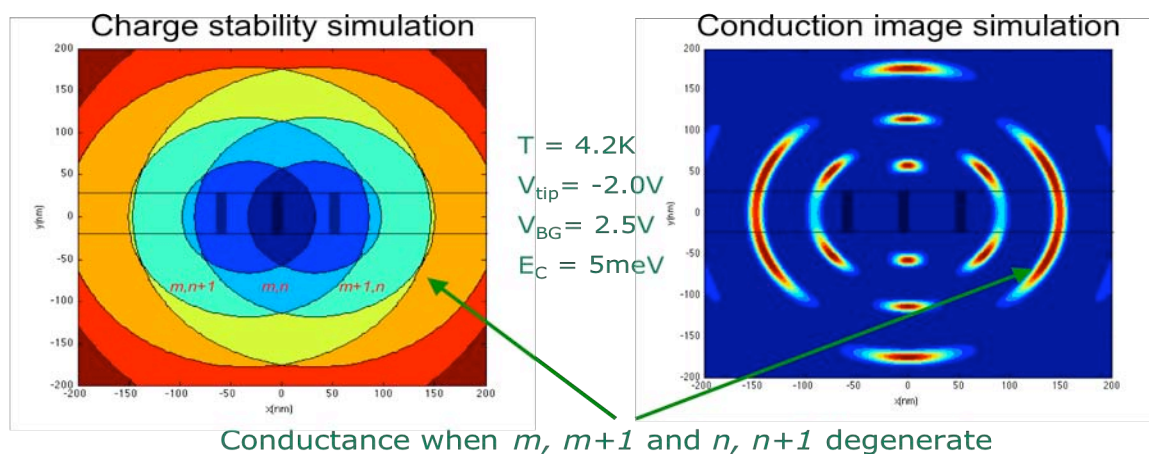


Figure 3.8. Simulations: (*left*) Charge stability — integer number m and n of electrons in each quantum dot vs. tip position. The charging diagram for each dot is a bullseye, and the offset between dots allows one to individually tune the charge on each dot with the tip. (*right*) Conduction image — the conduction through the double dot is shown vs. tip position. The Coulomb blockade conductance is large only for tip positions that allow the charge on both dots to change, at the intersections of the bullseye rings on left. The location of the nanowire dots are shown. The parameters are: temperature T , tip voltage V_{tip} , back gate voltage V_{BG} , and charging energy E_C .

patterns for the two dots overlap. In the experiments, this pattern of peaks will define the charging diagram.

These simulations show that an SPM tip can be used to individually control the charge on each dot in a double dot structure via its position. This approach will allow us to conduct a full range of experiments to manipulate the charge and spin on double dots grown inside heterostructure nanowires.

Photonic Devices Based on GaN Nanowires

Venkatesh Narayanamurti

Applied Physics and Physics, Harvard University

Collaborators: Federico Capasso, Shriram Ramanathan (Harvard University); Arthur C. Gossard (University of California, Santa Barbara); L.R. Ram Mohan (Worcester Polytech Inst.)

A. Research on Gallium Nitride Nanowire Heterostructure Photonic Devices

In the past year, close collaborations with Federico Capasso has been carried out for the purpose of studying Gallium Nitride (GaN) nanowire-based photonic device applications and modeling, as part of our continuous efforts in nanowire research. The hydride vapor phase epitaxy (HVPE) and chemical vapor deposition (CVD) growth of GaN nanowires and their physical properties, including TEM, photoluminescence, and electronic transport, have been established in our group under a previous NSF grant.

HVPE and CVD Growth of GaN

GaN nanowires are technologically attractive due to a promising combination of the electronic and optical characteristics of GaN with the one-dimensional confinement offered by the nano-scale wire structure. Among the nanowire growth modes, catalytic growth (vapor-liquid-solid) is commonly favored for the certain degree of control it offers over wire size and position.

In GaN film growth, HVPE presents several advantages over the more common metal-organic vapor growth methods, such as high growth rates of over 100 $\mu\text{m}/\text{hour}$ and carbon-free/self-cleaning, resulting in high quality GaN with record high mobility.

For nanowire growth, HVPE presents very specific challenges. The fast growth rate presents a strong competition between direct vapor growth (usually undesired as it tends to thicken the wires) and the desired vapor-liquid-solid catalytic growth mode. Furthermore, the HCl produced in the reaction of GaCl and ammonia tends to etch away the metal catalyst. Hence, the only report to date on HVPE growth of GaN nanostructures was not catalytic (no ability to define or pattern the growth site) and was of limited aspect ratio. In 2005, we reported on a first successful attempt at catalytic growth of large aspect ratio GaN nanowires [1,2].

In parallel with the HVPE effort, we also studied CVD growth of GaN. The advantage of CVD has proven to be in the wire size. HVPE is known to yield a very fast growth rate, with which there is a tight competition between the preferred catalyzed mode and the direct vapor growth, commonly resulting in thick wires (more than 100 to 200 nm). In CVD the difference between the direct and catalyzed growth rates enables us to obtain typically thinner wires at the range of 30 to 50 nm.

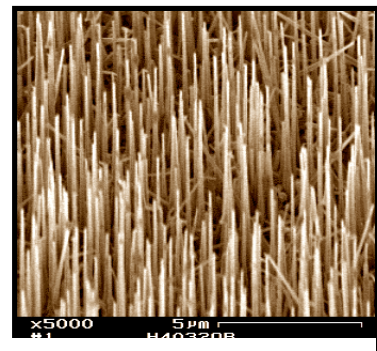


Figure 3.9. Vertically aligned HVPE-grown GaN nanowires on sapphire substrate.

Photonic Device Applications and Modeling

The most basic photonic device generally attempted in nanowires is the light emitting diode. Once electroluminescence can be routinely achieved, one can move further on into electrically pumped nanowire lasers. Many future applications, such as integrated photonics, rely on the miniaturization and integration of LEDs of different colors on a single chip. A viable avenue to achieve this is the use of semiconductor nanowires. Nanowires of the group III nitrides are especially attractive candidates given that their emission wavelength can be tuned from the infrared—Indium Nitride—to ultraviolet—Gallium Nitride—through variations in alloy composition. Gallium Nitride (GaN) is the most mature of them, i.e., the backbone of the family, which serves as the base for most of the published applications to date.

So far, electroluminescence (EL) from GaN nanowires has been reported in several device configurations, in a cross-wire geometry, in single nanorod axial p-n junctions, and in radial core/multishell heterostructures. However, in all of these approaches carrier injection is generally limited to a small fraction of the semiconductor material, which limits the output power. A more efficient architecture would make use of the entire length of the nanowire cavity for current injection, which, together with proper feedback, could also be suitable for nanowire lasing. In collaboration with Capasso group, we reported electroluminescence from a hybrid structure composed of a n-type GaN nanowire in contact with a p-type Si substrate, where the current is injected along the length of the nanowire. This scheme is attractive for several reasons. First of all, it does not require complex nanowire growth techniques involving either axial or radial dopant modulation. Second, it can be applied to materials that are poor amphoteric semiconductors, i.e., semiconductors that are difficult to obtain in both n- and p-type. Finally, device assembly does not require complicated fabrication steps, as is the case with core/multishell heterostructures (e.g., selective etching of the nanowire shell to contact the core). As we showed, our structure emits ultraviolet EL from the GaN band edge under both bias polarities, suggesting that light emission is mediated by *tunnel-injection* of carriers through thin native oxide barriers. This work therefore provides strong evidence that the standard commonly invoked p-n junction model is generally not applicable to this kind of device structure [3].



Figure 3.10. Light-emitting diode made of n-type GaN nanowire on a p-type Si substrate (Cover of Nanotechnology Journal).

If the mechanism is indeed tunneling, the device should also work, if we replace the p-type substrate with an n-type one. Indeed, electroluminescence from a heterostructure device made of n-type GaN nanowire on n-type Si substrate was also observed. A novel feature of this device is that by reversing the polarity of the applied voltage the luminescence can be selectively obtained from either the nanowire or the substrate. For one polarity of the applied voltage, ultraviolet (and visible) light is generated in the GaN nanowire, while for the opposite polarity infrared light is emitted from the Si substrate.

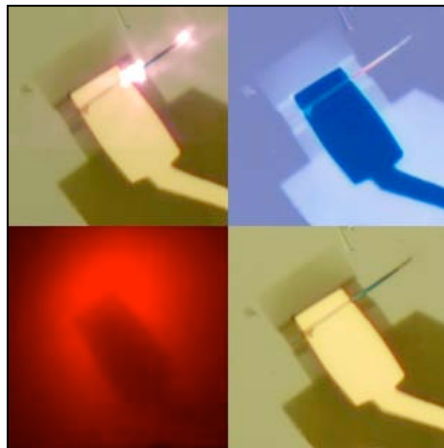


Figure 3.11. Light-emitting diode made of n-type GaN nanowire on a n-type Si substrate (bottom right), showing different light emission under forward (top left) and reverse (bottom left) bias.

We proposed a model, which explains the key features of the data, based on electron tunneling from the valence band of one semiconductor into the conduction band of the other semiconductor. For example, for one polarity of the applied voltage, given a sufficient potential energy difference between the two semi-conductors, electrons can tunnel from the valence band of the GaN into the Si conduction band. This process results in the creation of holes in GaN, which can recombine with conduction band electrons generating GaN band-to-band luminescence. A similar process applies under the opposite polarity for Si light emission. This device structure affords an additional experimental handle to the study of electroluminescence in single nanowires and, furthermore, could be used as a novel approach to two-color light-emitting devices [4].

References

- [1] G. Seryogin, I. Shalish, W. Moberlychan, and V. Narayanmurti, "Catalytic hydride vapor phase epitaxy growth of GaN nanowires," MRS Fall Meeting, Boston (2005).
- [2] G. Seryogin, I. Shalish, W. Moberlychan, and V. Narayanmurti. "Catalytic hydride vapor phase epitaxy growth of GaN nanowires," *Nanotechnology* **16**, 2342 (2005).
- [3] M.A. Zimmler, J. Bao, I. Shalish, W. Yi, J. Yoon, V. Narayanamurti, and F. Capasso., "Electroluminescence from single nanowires by tunnel injection: An experimental study," *Nanotechnology* **18**, 235205 (2007).
- [4] M.A. Zimmler, J. Bao, I. Shalish, W. Yi, V. Narayanamurti, and F. Capasso, "Two-color heterojunction unipolar light-emitting diode by tunnel injection," *Nanotechnology* **18**, 395201 (2007).

B. UHV – Dual Tip STM/BEEM (Marissa Olson-Hummon, Andrew Stollenwerk)

A new dual probe scanning tunneling microscope (STM) with single photon collection capabilities has been designed, machined and assembled. An ultrahigh vacuum (UHV) chamber has been designed for this microscope. This chamber has proven to reach pressures below 3×10^{-11} torr, making it more than adequate for UHV experiments. In addition, the microscope has two sample contacts for possible four probe measurements and a cold finger for low temperature ~ 100 K measurements (untested).

Preliminary results have been obtained using platinum-iridium tips on a graphite sample. The spectroscopy acquired from this sample displays the characteristic exponential dependence of voltage to current associated with tunneling. Scanning has been achieved on the graphite sample in atmosphere. In the future, integration of the microscope with the UHV chamber will allow scanning in UHV. Specially designed sample holders will allow tips to be transferred *in situ*. Initial tests will be performed on silicon (111), prepared in a separated UHV chamber and transferred to the microscope without breaking vacuum. The ultimate goal of the STM is to measure tunneling induced luminescence from cadmium selenide (CdSe) nanocrystals (NCs) in several different dielectric environments. Comparing the measurement at room temperature and 100K will help us identify the role of hopping conduction through the medium surrounding the CdSe NC with regards to its luminescence efficiency.

C. Study of Structure-Property Relationships in VO₂

Rf-sputtered VO₂ films grown by Shriram Ramanathan have been studied by a joint postdoctoral fellow (D. Ruzmetov). In particular the phase transition in the neighborhood of 70°C has been studied as a function of growth conditions. Sharp turn on in the resistivity of these thin films has been observed and correlated with structural and X-ray PES studies. Recently the IR reflectivity has been shown to go from insulator to metal and be consistent with a percolation model for the phase transition.

Theory of Electron and Spin Transport in Nanostructures

Bertrand I. Halperin

Physics, Harvard University

Collaborators: Arthur C. Gossard (University of California at Santa Barbara); Robert M. Westervelt, Charles M. Marcus, Amir Yacoby (Harvard University)

International Collaborators: Arne Brataas (Norwegian University of Science and Technology), Leo Kouwenhoven (Delft University of Technology)

The overall goal of this work is to gain a better understanding of the electronic structure of nanoscale building blocks, and of the operations of nanoscale devices, in order to improve our ability to design and construct such devices. A crucial aspect of the development of new structures and devices are measurements to characterize these structures. Theoretical efforts are necessary to understand the results of such measurements as well as to suggest new types of measurements as well as possible improved structures. Our projects are motivated by NSEC supported experiments including particularly measurements of transport in semiconducting nanowires, and imaging of electron flow and electronic states in structures made from two-dimensional electron systems. Goals include development of theoretical and calculational techniques, as well as applications to specific systems.

Nanowires. InAs nanowires are a particularly interesting system for fabrication of nanoscale semiconductor devices, and they are being actively studied in laboratories of the Westervelt and the Kouwenhoven groups, among others.[1] We are trying to understand the electronic states in these wires, and trying to see how much information one may gain by analyzing transport in the presence of an inhomogeneous gate potential. We are also interested in effects of an applied magnetic field. Electron-electron interactions play a central role in our analyses.

In 2007, graduate student Jiang Qian, working together with B.I. Halperin, completed a Hartree-Fock study of electrons in a one-dimensional wire with a central region of reduced electron density, produced by an external gate [2]. This work was motivated in large part by experimental work in the laboratory of Amir Yacoby, using transport and tunneling techniques, on quantum wires produced by the cleaved-edge overgrowth technique in GaAs heterostructures [3]. However, the calculational techniques, and many of the results, should be applicable as well to InAs nanowires in the regime accessible to imaging experiments in Westervelt's laboratory [1].

A main focus of the Hartree-Fock work was to investigate the situation where the region under the central gate has very low electron density, so that electron-electron interactions become large compared to the kinetic energy, and the system approaches a Wigner-crystal like regime. Within the Hartree-Fock approximation, an infinite wire will develop a periodic charge modulation, with an antiferromagnetic ordering of spins, at moderately low densities. At very low densities, there will be a phase transition to ferromagnetic order, in the absence of an applied magnetic field. The ferromagnetic order is, strictly speaking, an artifact of the Hartree-Fock approximation, since it is known that

the exact ground state in zero field will always have total spin zero and have antiferromagnetic correlations, which fall off proportional to the inverse of the spatial separation. However, the Hartree-Fock calculation may be a good representation of the physics in the presence of an applied magnetic field.

The situation becomes more interesting, and non-trivial, when the low-density region has finite length and is joined smoothly to regions of high electron density, outside the gate. Our calculations show the development of Wigner-crystal-like order in the central region when the electron density there becomes sufficiently low, with a central sequence of electrons whose spin becomes aligned to the applied magnetic field. As the gate voltage is increased, electrons leave the spin-aligned central region one by one, leading to steps in the density, much as one would have for a quantum dot separated by a tunnel barrier from an attached lead. (Here, however, the central region is strongly coupled to the surrounding region, with an applied potential that decreases monotonically into the leads.) These results are in good agreement with the experiments in Yacoby's laboratory [3].

Hartree-Fock calculations are numerically considerably more difficult than the more standard Local Density Approximation (LDA) calculations, but we believe they are more realistic for a one-dimensional system with low electron density and large density gradients, where spin correlations may be important. Our calculations have included up to 1000 electrons overall in the quantum wire.

Spin-orbit effects. Spin-orbit effects on transport in semiconductor systems have been a major focus of interest over a period of years, as analysis has shown a remarkable subtlety in these problems. The work supported by NSEC has concentrated on effects of confinement in small quantum dots and phenomena at a boundary or interface between 2-D regions with different spin-orbit coupling.

In one project, supported by NSEC, Halperin and his student Jacob Krich have investigated the effect of the k^3 Dresselhaus coupling (i.e., the spin-orbit coupling term proportional to the cube of the electron momentum k) on transport through a two-dimensional ballistic quantum dot [4]. Although the k^3 term should have negligible effect in very small dots, and should be less important than k -linear terms in large dots, calculations show that the term can be dominant in dots of intermediate size, as were studied several years ago in the laboratory of Marcus (in a collaboration involving Gossard) [5]. Combining these experimental results with our theoretical analysis indicates that the coupling constant for the k^3 term is at least a factor of two smaller than the value that has been most commonly assumed in earlier papers, but is consistent with the smallest values that have been previously proposed.

In another work, supported by NSEC, Halperin and collaborators Tserkovnyak, Kovalev, and Brataas, have studied the boundary spin Hall at a transmitting interface between two-dimensional electron systems with different values of the Rashba coupling constant [6] Such an interface could be produced by putting a gate over one half of the sample, and applying a voltage to the gate, changing the well-asymmetry and the electron

density under the gate. We have found that the boundary condition for the coupled equations governing spin generation, flow, and diffusion, in the presence of an electric current parallel to the interface, depends in a surprising way on the variation in the electron mobility near the boundary, as well on the variation in Rashba coupling constant. In the simplest case, where the mobility is a constant, and the Rashba coupling vanishes on one side of the interface, we find no spill-over of the spin polarization and no spin injection into the non-spin-orbit phase, in contradiction to predictions that appeared previously in the literature.

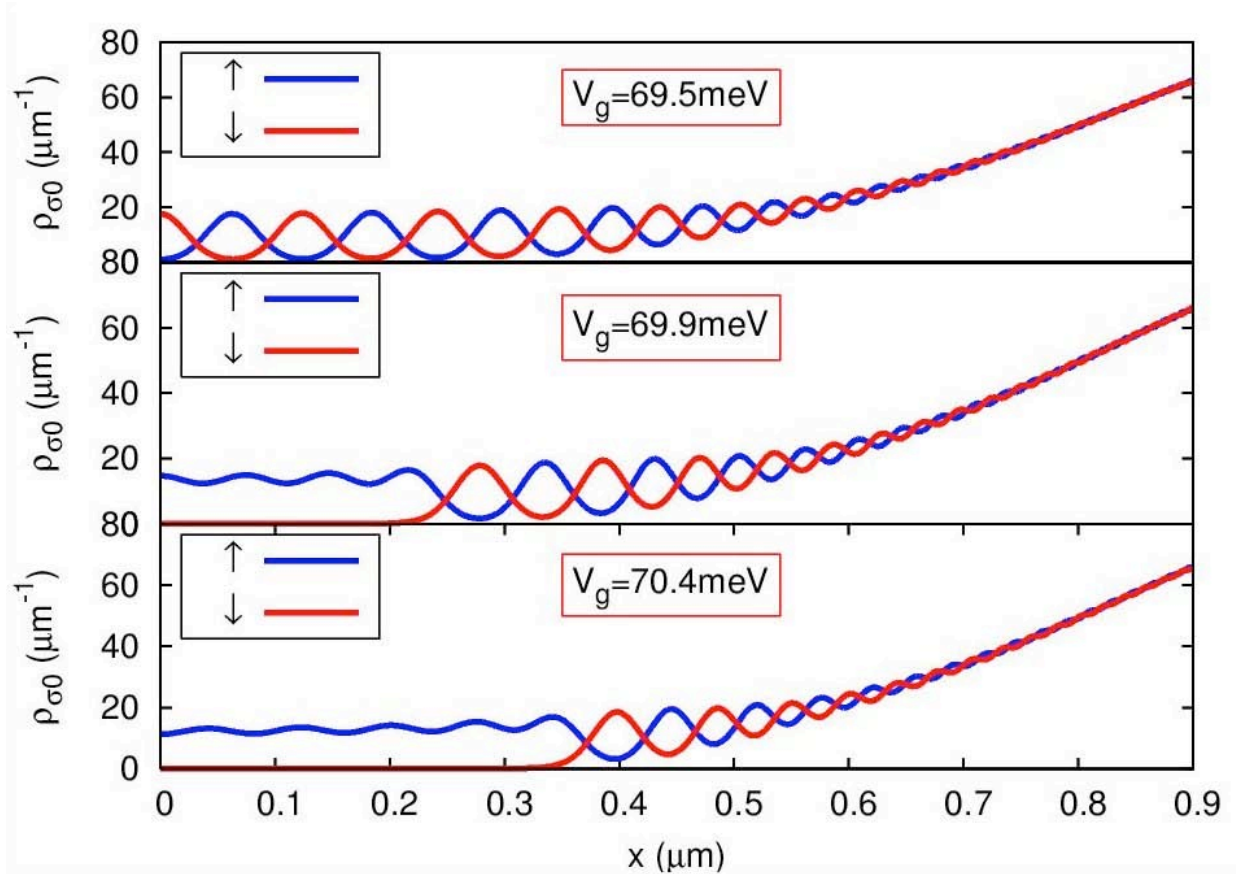


Figure 3.12. Densities of spin-up and spin-down electrons, as a function of position, in a one-dimensional quantum wire, with reduced density near the center due to the influence of a repulsive external gate. Results are obtained from a Hartree-Fock calculation. Note the transition from antiferromagnetic spin-order to complete spin alignment, in the central region, as the gate potential is increased and the electron density is further reduced. System is symmetric about $x = 0$.

Another project with NSEC support, a collaboration between Halperin and theorists at MIT and Brookhaven National Laboratory, has shown how spin-orbit coupling can lead to measurable non-local conductance effects, mediated by spin diffusion [7].

Several other projects involving spin-orbit coupling were primarily supported by another grant, but received some support from NSEC. These resulted in a paper on the production of out-of-plane spin polarizations from in-plane electric and magnetic fields in a semi-conductor system, and another paper on spin-generation by nonlinear transport, away from the boundaries of a sample [8,9]. The first paper, written by Engel, Rashba,

and Halperin was published in *Physical Review Letters* during 2007, while the second, written by Halperin's student Ilya Finkler, together with Halperin, Engel, and Rashba, was published in *Physical Review B*. A review article on the theory of spin Hall effects in semiconductors, written by Engel, Rashba, and Halperin, was published in 2007 in the *Handbook of Magnetism and Advanced Materials* [10].

References

- [1] A.C. Bleszynski, F.A. Zwanenburg, R.M. Westervelt, A.L. Roest, E.P.A.M. Bakkers, and L.P. Kouwenhoven, "Scanned probe imaging of quantum dots inside InAs nanowires," *Nano Lett.* **B**, 2559 (2007).
- [2] J. Qian, B.I. Halperin, "Hartree-Fock calculations of finite inhomogeneous quantum wire, arXiv:0707.2992; *Phys. Rev. B* (in press).
- [3] O.M. Steinberg, O.M. Auslaender, A. Yacoby, J. Qian, G.A. Fiete, Y. Tserkovnyak, B.I. Halperin, K.W. Baldwin, L.N. Pfeiffer, and K.W. West, "Localization transition in a ballistic quantum wire," *Phys. Rev.* **B73**, 113307 (2006).
- [4] J.J. Krich, B.I. Halperin, "Cubic Dresselhaus spin-orbit coupling in 2D electron quantum dots, *Phys. Rev. Lett.* **98**, 226802 (2007).
- [5] D.M. Zumbuhl, J.B. Miller, C.M. Marcus, D. Goldhaber-Gordon, J.J.S. Harris, K. Campman, and A.C. Gossard, *Phys. Rev.* **B72**, 081305(R) (2005).
- [6] Y. Tserkovnyak, B.I. Halperin, A.A. Kovalev, and A. Brataas, "Boundary spin Hall effect in a Rashba semiconductor," *Phys. Rev.* **B76**, 085319 (2007).
- [7] D.A. Abanin, A.V. Shytov, L.S. Levitov, B.I. Halperin, "Nonlocal charge transport mediated by spin diffusion in the Spin-Hall effect regime," arXiv:0708.0455.
- [8] H.-A. Engel, E.I. Rashba, and B.I. Halperin, Out-of-plane spin polarization from in-plane electric and magnetic fields, *Phys. Rev. Lett.* **98**, 036602 (2007).
- [9] I.G. Finkler, H.A. Engel, E.I. Rashba, and B.I. Halperin, "Spin generation away from boundaries by nonlinear transport," *Phys. Rev.* **B75**, 241202 (2007).
- [10] H.-A. Engel, E.I. Rashba, and B.I. Halperin, Theory of spin Hall effects in semiconductors, in *Handbook of Magnetism and Advanced Magnetic Materials*, H. Kronmüller and S. Parkin, eds. (John Wiley & Sons, Chichester, UK, 2007) vol. 5, pp 2858–2877.

Scanning SET Imaging of Graphene

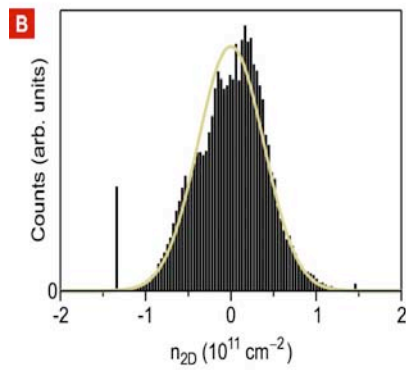
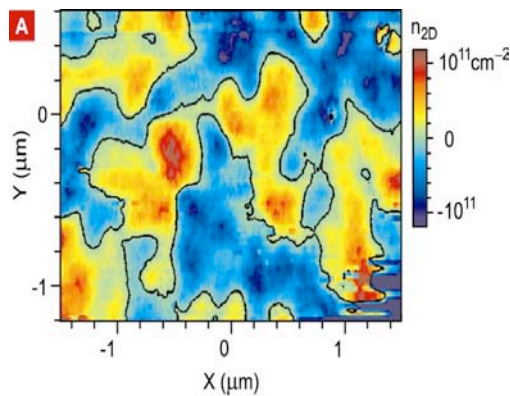
Amir Yacoby

Physics, Harvard University

Collaborator(s): Bertrand I. Halperin (Physics, Harvard)

Research Goal, Approach and Accomplishments.

The electronic density of states of graphene is equivalent to that of relativistic electrons. In the absence of disorder or external doping the Fermi energy lies at the Dirac point where the density of states vanishes. Although transport measurements at high carrier densities indicate rather high mobilities, many questions pertaining to disorder remain unanswered. In particular, it has been argued theoretically, that when the average carrier density is zero, the inescapable presence of disorder will lead to electron and hole puddles with equal probability. In this work, we used a scanning single electron transistor to image the carrier density landscape of graphene in the vicinity of the neutrality point. At zero external magnetic field our results clearly show (Figure 3.13) the electron-hole puddles expected theoretically. The typical puddle size is limited by our resolution and the density variations are approximately $3.9 \times 10^{10} \text{ cm}^{-2}$. In order to determine the intrinsic magnitude of the disorder we look at the inverse compressibility in the presence of a magnetic field. The width in density of the Landau levels shown in Figure 3.14 provides a direct measure of the disorder in density (found approximately to be $2 \times 10^{11} \text{ cm}^{-2}$). The two measures of disorder yield an estimate of the disorder length scale given by approximately 25 nm. In addition, our measurement technique enables to determine



locally the density of states in graphene. In contrast to previously studied massive two-dimensional electron systems, the kinetic contribution to the density of states accounts quantitatively for the measured signal. Our results suggest that exchange and correlation effects are either weak or have canceling contributions.

Figure 3.131. (A) Color map of the spatial density variations in the graphene flake extracted from surface potential measurements at high density and when the average carrier density is zero. Blue regions correspond to holes and red regions to electrons. The black contour marks the zero density contour. (B) Histogram of the density distribution in Figure 1(A).

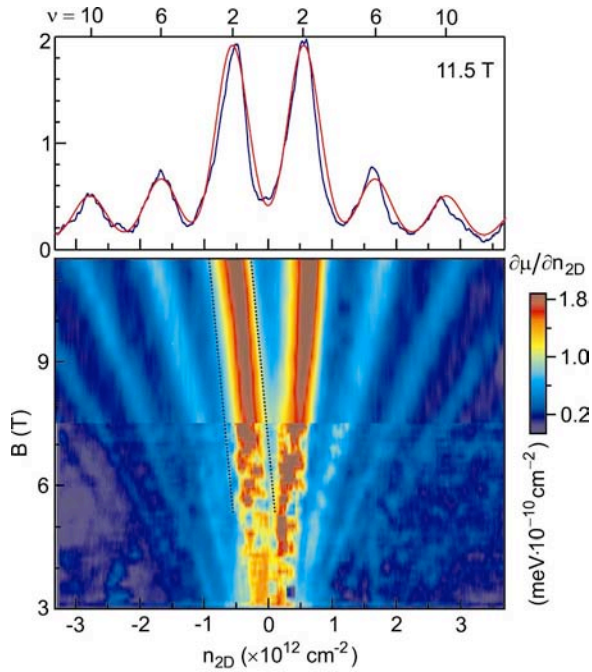


Figure 3.14. (A) Color rendering of the inverse compressibility as a function of density and magnetic field. (B) A single line scan from plot A of the measured inverse compressibility (black line) at a magnetic field of 11 T. The red curve is a fit to the data composed of Gaussians with equal variance for each maximum. This variance measures the width of the incompressible regions (maxima) centered around integer fillings and provides an estimate for the intrinsic amplitude of the density fluctuations.

Imaging Spins in Quantum Dots

Marc A. Kastner

Physics, Massachusetts Institute of Technology

Collaborators: Arthur C. Gossard (University of California at Santa Barbara); Charles M. Marcus, Robert M. Westervelt (Harvard University); Loren Pfeiffer (Bell Labs/Alcatel-Lucent Technologies); Ya-Hong Xie (University of California at Los Angeles)

The long-range goal of our NSEC work is to image electron spins in quantum dots. Westervelt's group has made great advances in imaging electron charge density. Imaging the spin density of electrons in nanostructures will give additional information about electronic wave functions and may be useful in characterizing devices, for quantum computing for example. Our paper showing that single electron spins in quantum dots can remain in the excited state for very long times, over 1 sec, has recently been published. This makes spin manipulation more promising.

During this study we made a remarkable discovery. In a magnetic field parallel to the two-dimensional electron gas, electrons can tunnel into either the ground or excited spin state. Theory predicts that the tunneling rates for these two processes should be the same. However, we observe a large difference between the two rates.

We measure the tunneling rates by monitoring the charge on the quantum dot with a nearby quantum point contact (QPC) (see Fig. 4.15a.). Figures 3.15b and 3.15c illustrate how we manipulate charge and spin on the dot. We first empty the dot (ionize) by applying a pulsed negative voltage to one of its gates, which raises the energy of the one electron in the dot above the Fermi energy of the nearby lead. We then apply a less negative voltage for a short time (load), during which an electron can tunnel from the lead onto the dot. We use the QPC to determine whether or not the tunneling event takes place, and by repeating the process many times, for fixed values of the voltage during the tunneling back onto the dot, we can determine the tunneling rate (Fig. 3.15d). We then plot the rate as a function of the voltage (Fig. 3.15e). This clearly shows the contributions from the two spin states.

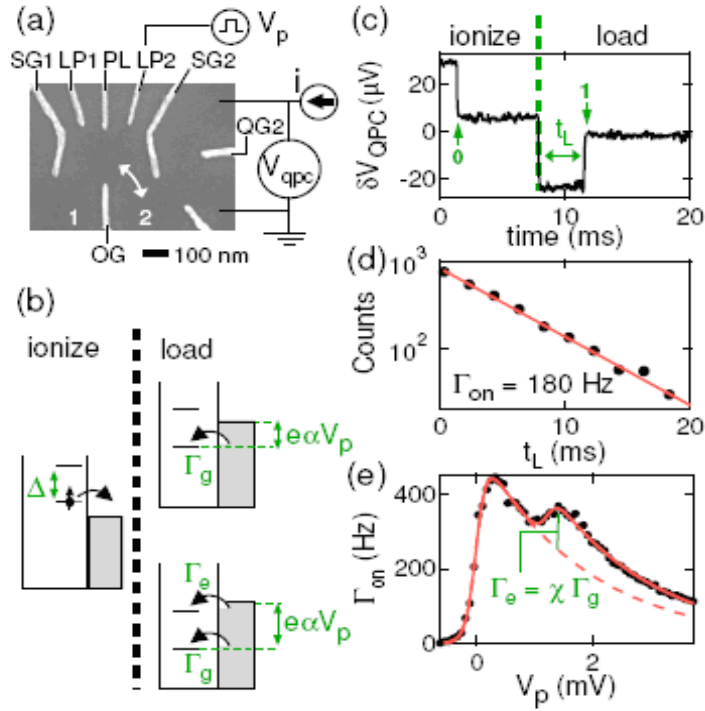


Figure 3.15. (a) Electron micrograph of the gate geometry. Negative voltages are applied to the labeled gates while the unlabeled gate and the ohmic leads are kept at ground. Voltage pulses of size V_p are applied to gate LP2. (b) Dot energy diagrams showing the position of the spin states during the pulse sequence. (c) Example of real-time data. The direct capacitive coupling between LP2 and the QPC causes the QPC to respond to the pulse sequence; electron tunneling events are evident on top of this response. The 0 denotes when an electron tunnels off the dot, while the 1 denotes when an electron tunnels on. (d) Example of a histogram of t_L for a given pulse depth. Fitting these data to an exponential (solid line) gives Γ_{on} . (e) Γ_{on} as a function of pulse depth V_p at $B = 5$ T. Fitting the data allows one to extract the ratio of the rate for the excited state to that of the ground state, $\chi = \Gamma_e / \Gamma_g$.

The surprise is shown in Figure 3.16. In the lower left panel of the figure we see the behavior predicted by theory. As we make the voltage less negative, we first see a peak in the tunneling rate when the ground state becomes degenerate with the Fermi energy in the lead, and then a second peak for the excited state. The red curve is the prediction of theory with equal tunneling rates for the two states. This is what is observed at low magnetic field. However, at high magnetic field we observe the rates in the lower right panel. We observe the peak for the ground state, but that for the excited state is strongly suppressed. The upper panel shows how this suppression depends on magnetic field.

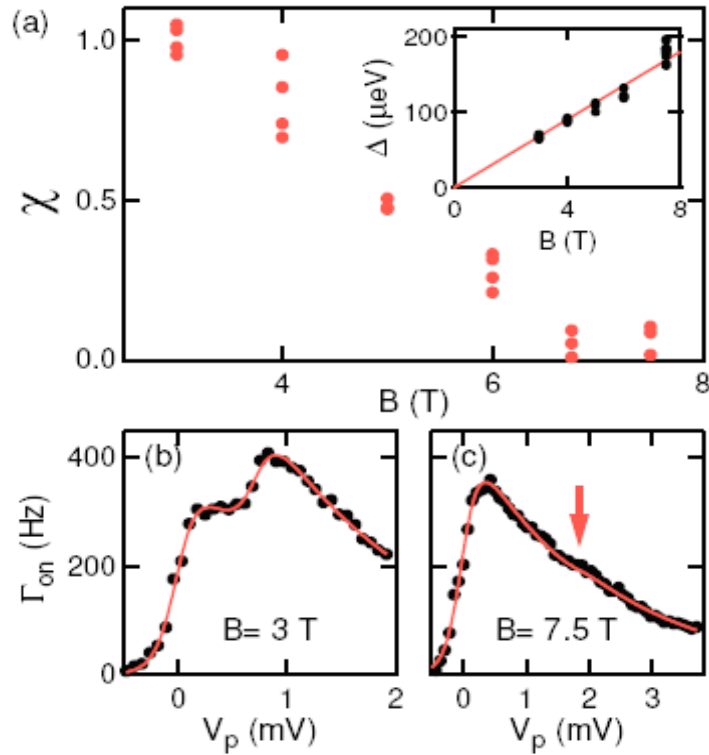


Figure 3.16. (a) χ as a function of magnetic field from fits to data such as those in Figure 1(e). The inset shows the spin splitting as a function of magnetic field. (b) Data and the best fit at $B = 3$ T. The increase in the tunneling rate caused by the excited spin state passing below the Fermi energy is clearly visible. (c) Data and fit at $B = 7.5$ T. The arrow marks the value of V_p where the feature is expected to be.

We have also found that this spin-dependent tunneling is very sensitive to the shape of the quantum dot. While this implicates spin-orbit coupling, the known strength of the coupling appears to be too small to account for the observed effects. This shape dependence shows that imagining of the spin distribution would be very interesting. A manuscript reporting our work has been submitted for publication.

Our effort in the next year will focus on the fabrication and study of quantum dots in Si quantum wells. These should have a much longer phase decoherence time T_2 than GaAs because of the smaller hyperfine coupling and the lower density of nuclear spins. Our efforts to make dots have not yet been successful. We believe that this is the result of incomplete depletion under our gates at voltages that have acceptable leakage of the Schottky barriers. We are using MBE-grown Si quantum wells, and it is well-known that the layers above the Si are prone to leakage. We have minimized this, following the work of the Eriksson group, by making the gate area on the mesa as small as possible. On the other hand, one cannot make the gates too narrow, or depletion will be inadequate. Another round of fabrication is likely to yield working devices.

If we can measure the relaxation times in the Si quantum well, we will encourage our collaborator Xie to grow quantum wells with isotopically pure Si, which should have T_2 of the order of T_1 . Since there will be very weak spin-orbit coupling, these times could be extremely long.

Nanoparticle-Based Molecular Imaging via MRI

Charles M. Marcus

Physics, and Center for Nanoscale Systems, Harvard University

Collaborator: David Cory (MIT)

Statement of Project. We are developing a class of nanoparticle imaging agents (NIA's), functionalized with macromolecules such as monoclonal antibodies (mAb) to form nanobiological hybrid materials that can be tracked within the body using magnetic resonance imaging (MRI). The core material, a type of silicon, is biologically inert before functionalization, inexpensive, and readily available, having been developed for application in the semiconductor industry.

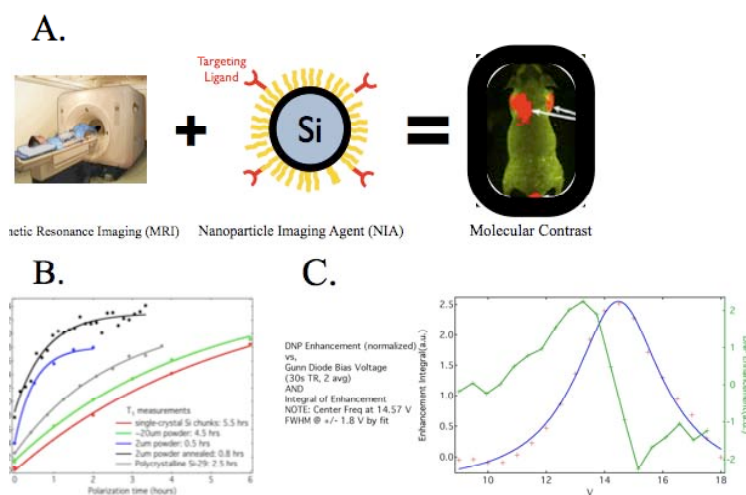


Figure 3.17.

A. Schematic picture of NIA-MRI;

B. Preliminary polarization recovery (T_1) data for silicon micro-particles at a variety of sizes;

C. Dynamic nuclear polarization (DNP) observed in silicon nanoparticles. Data is consistent with the Thermal Mixing mechanism of DNP.

Course of Investigation. The research for the NIA-MRI project has fallen into three primary categories: (1) the solid-state physics underlying Dynamic Nuclear Polarization (DNP) of silicon; (2) the surface chemistry involved with attaching biologically compatible and biologically active ligands to silicon nanoparticles; (3) the material science for producing nanoparticles with properties optimized both for DNP and for biological targeting.

Under Category 1, we have designed and constructed two apparatuses for nanoparticle DNP, each optimized for different applications of our NIA. The first apparatus is optimized for techniques well understood for low-temperature ($T = 4$ degrees Kelvin), high-field (3 tesla) DNP of solids. In this embodiment, NIA-MRI would entail

ex vivo DNP of the nanoparticles to enhance the MRI signal arising from the nanoparticles themselves by several orders of magnitude ($> 3000\times$), removing the nanoparticles from the low-temperature apparatus and injecting them into live animal (see Figure 3.17A). Feasibility of this technique of polarization has been demonstrated (Figure 3.17C) with collaborator Prof. David Cory (MIT). Additionally, very long polarization recovery times of >1 hr (Figure 3.17B) accommodate moderate time delays required for re-warming and suspension of NIA prior to injection.

The second apparatus designed and constructed under Category 1 is optimized for *in vivo* DNP and direct imaging at low field. Applications of this system include longitudinal tracking of NIA for times much longer than T_1 , which will require re-polarization *in vivo*. Both apparatuses consist of home-built, highly flexible consoles and electronics.

Under Category 2, we have reached preliminary functionalization goals for the nanoparticle agents. This has included amination of oxidized (SiO_2) surfaces using an aminopropyltriethoxysilane (APTES) linker molecule, and the subsequent conjugation of polyethyleneglycol (PEG) to that surface. This technique, known as “PEG-ylation” is a critical intermediate step to the conjugation of complex and target-able ligands to the NIA surface. Additionally, PEG coatings are known to substantially reduce immune response to nanoparticles, both increasing the circulation lifetime *in vivo* and to reduce toxicity to living cells. Validation studies are ongoing.

Under Category 3, we have worked with the Center for Nanoscale Systems to develop a nanoparticle synthesis facility as well as systematic methods for categorizing the relevant material properties to our investigation. This has included techniques for grinding bulk silicon while minimally perturbing the underlying crystalline structures necessary for DNP, controlled oxidation of the nanoparticles surfaces to prevent accumulations of defects which may compromise both PEG-ylation and the polarization recovery times, separation by centrifugation of nanoparticles into narrow distributions of sizes and characterization of nanoparticle size distributions both by scanning electron microscope (SEM) and dynamic light scattering (DLS) measurements.

Simulations of Electrons in Nanowires and Coupled Quantum Dots

Michael Stopa

Center for Nanoscale Systems, Harvard University

Collaborators: Normand Modine (Sandia Nat. Lab.); Seigo Tarucha (University of Tokio)

Research Goal, Approach and Accomplishments. My research goal is to use numerical and analytic methods and models to describe and predict the properties of nanoscale systems such as nanowires, quantum dots and molecules. Many of the properties which I investigate are best approached from a simulations and modeling perspective. In this context I have developed a simulation code called “SETE” which calculates, within the effective mass, density functional method, the electronic structure of quantum dots, two-dimensional electron gas (2DEG) layers, semiconductor nanowires and nanoparticles embedded in dielectric material. The particular foci of my recent work with this tool and with analytic methods include the following: (1) electronic structure of semiconductor nanowires, (2) electrical noise immunity of double quantum dots in 2DEG structures, (3) Förster coupling of excitons in nanocrystals embedded in dielectric medium. Each of these is described in turn in the following:

Semiconductor Nanowires

One of the driving motivations behind nanoelectronic research is the concern that the progress of microelectric integration summarized by Moore’s Law may be coming to an end. For approximately forty years the density of circuit integration on manufactured

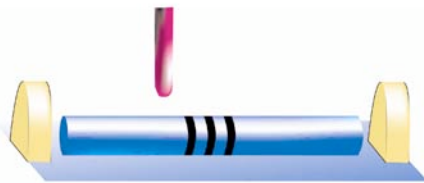


Figure 3.18. Illustration of semiconductor nanowire with leads and adjacent SPM tip.

microprocessors has doubled roughly every two years with a concomitant increase in the speed of these processors. The scaling down of gate size required to achieve this advance has been accomplished through improvements in lithography, changes of material composition and other methods. The limits of down-scaling simply by improved processing technology, however, may soon be reached when devices enter the quantum domain and the single charge domain. At this nanoscale, new device concepts and structures are assumed to be necessary. Semiconductor nanowires, which are grown to radii as small ~20 nm, have recently been developed and are a promising route for future device technology. The development of this promising technology, however, is hindered by the complexity of the material system. Multiple facets (as opposed to a simple wafer surface), strain and quantum confinement effects all require measurement and, more germanely, simulation to

microprocessors has doubled roughly every two years with a concomitant increase in the speed of these processors. The scaling down of gate size required to achieve this advance has been accomplished through improvements in lithography, changes of material composition and other methods. The limits of down-scaling simply by improved processing technology, however, may soon be reached

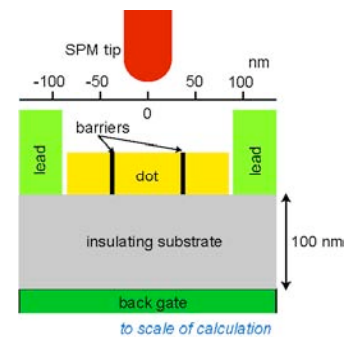


Figure 3.19. Scale drawing of simulation dimensions.

understand their influence on the transport through these nanowires.

I have employed the SETE program as a basis to the creation of a nanowire SETE which models the electronic structure of semiconductor nanowires. In addition, the inclusion of the tip of a scanning probe microscope into the simulation, as has been recently achieved experimentally by the Westervelt group and others, has added to the usefulness of the code in comparing with experiment.

Electrical Noise Immunity in Double Quantum Dots

Semiconductor quantum dots have proved to be valuable systems for studying the interaction of a small number of electrons in controllable environments. Transport properties and charge sensing techniques have developed to where the investigation of pairs of dots, each containing a single electron, has become possible. Such a system is the artificial equivalent of molecular hydrogen. This system in particular has been proposed as a possible basis for the implementation of quantum computation. The degree of control

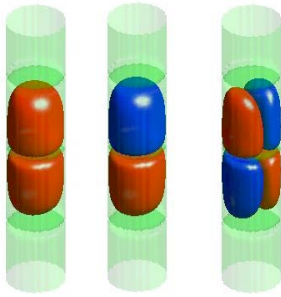


Figure 3.20. Sample wave functions of nanowire double dot.

required to achieve quantum computation, however, has not yet been reached and the experimental efforts have been concerned chiefly with controlling the coherent properties of the few electron system. In that context, coherence of electronic systems, even at very low temperatures (the experiments are performed at millikelvin temperatures) is very fragile. Since spin is used as the unit of information, the spin decoherence time (which is much longer than the electronic decoherence time) is the metric of importance. This decoherence is affected by fluctuations in the nuclear environment (through the hyperfine interaction) and also through fluctuations in the electrical environment, through charge or voltage noise. We have recently modeled the

electronic structure of artificial molecular hydrogen by combining a density functional approach for the basis states of the problem with a configuration interaction method for calculation of the correlated, interacting states of the system. The exchange interaction between the dots, which controls the mutual rotation of the dot spins, is normally very sensitive to slight fluctuations in the electrical environment. Through our simulations we were able to discover a “sweet spot” in the voltage-magnetic field parameter space where the exchange was, to lowest order, immune to charge or voltage fluctuations.

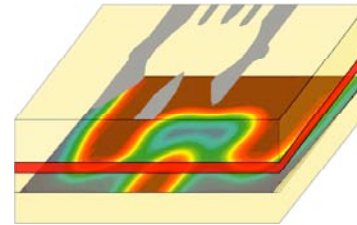


Figure 3.21. Schematic of double semiconductor quantum dot simulation and self-consistent potential at 2DEG level.

Förster Coupling of Excitons in Nanocrystals

A significant challenge for researchers in the field of alternative energy technology is the enhancement of the efficiency of light-gathering for photovoltaic cells. Recently it has been discovered that a layer of semiconductor nanocrystals adhering to the surface of a photovoltaic crystal can enhance the capture efficiency by possibly 30%. The process whereby excitons, upon being created by incident light, are moved from one nanocrystal

to an adjacent one (through a Coulomb mediated energy transfer without tunneling) is called the Förster effect. This effect, which has been known for fifty years, is also critical in the process of photosynthesis, so its clear understanding is of considerable importance.

We have been using simulations of the wavefunctions and energy levels of the excitonic state in the nanocrystal in a realistic environment (composed of metallic leads, gates and dielectric background matrix) to calculate the Förster transfer process in nanocrystals. Our earlier work on configuration interaction calculations in quantum dots has uncovered a method for calculating various Coulomb matrix elements without the need to do complicated, multi-dimensional integrals. Rather, we employ our solutions of Poisson Equation in the actual electrostatic environment to calculate these matrix elements and thereby automatically include the effect of screening by the gates and leads. This allows us, for the first time, to investigate an entire range of realistic geometries and hopefully will lead to the design of newer and even more efficient light gathering configurations of nanoparticles and surface elements for photovoltaic applications.

SEED: Single-Photon Photonic Device

Marko Lončar

Physics, Harvard University

Collaborator(s): Mounqi Bawendi (MIT)

Number of postdoctoral fellows: 0

Number of graduate students: 1

Number of undergraduate students: 0

Research Goal, Approach and Accomplishments. The goal of this project is realization of optical devices that operate at single photon level, including single-photon sources and switches, based on quantum emitters embedded in nanoscale optical cavities. For example, single photon source is a light source that emits photons one at the time, with extremely low probability of emitting multiple photons at the same time. A reliable and bright source of single photons would find immediate application in spectroscopy, quantum cryptography and quantum communication. Two main types of quantum emitters are being explored in our group: (i) Nitrogen-vacancy (NV) color centers in diamond, and (ii) semiconductor nanocrystals. At the same time, different optical cavities are being explored, including: (i) photonic crystal nanocavities, (ii) plasmonic nanostructures, and (iii) nanopillar cavities.

Single-Photon Sources Based on Diamond

Recently, it has been demonstrated that nitrogen-vacancy (NV) color centers in diamond are promising candidates for realization of single-photon sources and quantum registers [1–3]. In particular, it is important to emphasize their temporal and spectral

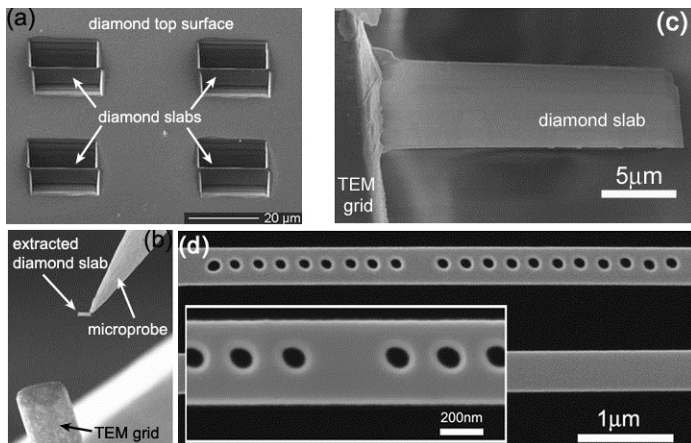


Figure 3.19. Fabrication of photonic crystal nanocavities in diamond membranes. (a) Vertical diamond slabs (~100 nm thick) are made using FIB milling. (b) The membranes are then extracted and (c) mounted onto TEM grid. (d) Finally, photonic crystal cavity is defined using FIB milling. SEM shows one of the first diamond nanocavities ever made in single-crystal diamond.

stability (no blinking, no spectral diffusion, etc.), as well as ability to deterministically position color centers using ion implantation. The luminescence spectrum on NV centers is broad (640 nm – 720 nm) with zero-phonon line at 640 nm, still visible at room temperature. In order to take full advantage of, and further enhance excellent properties of color centers, it is necessary to embed them into optical cavities. The purpose of the cavity is twofold: (i) It enhances the zero-phonon line emission and increase the rate of photon production (Purcell effect as large as $F_P > 1,000$), while suppressing phonon side-band, and (ii) facilitates collection of

single photons by channeling them into the well-defined cavity mode. Unfortunately, due to the difficulties associated with growth of high-quality, pure, single-crystal thin diamond films (~100 nm thickness), it has proven very difficult to realize high quality optical cavities using conventional nanofabrication techniques. This is the main reason why there is virtually no work in the field of diamond nanophotonics, in spite of tremendous promise offered by NV color centers embedded in optical nanocavities.

During the past year, we solved this problem using focused ion beam (FIB) milling and nanomanipulation, and we realized thin slabs of single crystal diamond (Figure 1). This important progress was entirely enabled by NSEC funding, and our work represents an important milestone towards realization of diamond nanophotonics and solid-state based quantum optics systems. The photonic crystal cavity shown in Figure 1(d), the world's first diamond nanocavity fabricated in single crystal diamond, is designed to

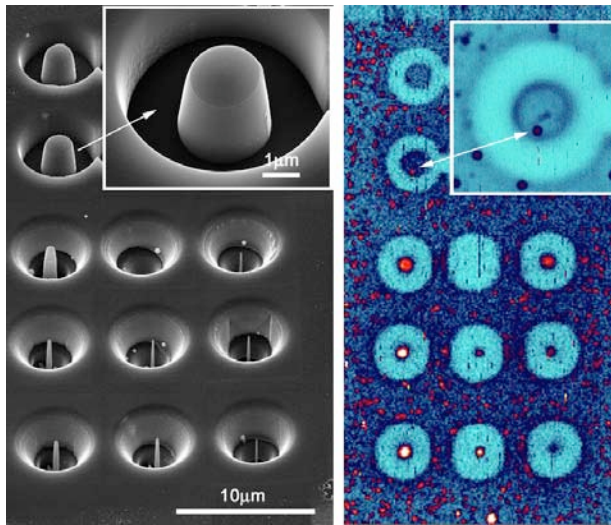


Figure 3.20. SEM micrograph of an array of diamond nanowires and microposts fabricated in single crystal CVD synthesized diamond. (b) Confocal photoluminescence image shows presence of single NV color centers (small red dots) inside nanowires, as well as in the large posts (inset).

operate at NV color center wavelength, and is expected to have quality factor $Q \sim 20,000$. The structures were fabricated in Harvard's shared nanofabrication facility operated by Center for Nanoscale Systems (CNS), part of NNIN. At present, we are characterizing our nanocavities, and validating the designs and fabrication procedure. During the previous year we have also built apparatus for experimental investigation of quantum-optical structures, based on confocal photo-luminescence. Our experimental setup is capable of spectrally- and time- resolved measurements of quantum emitters, at single photon level.

We are also investigation single-crystal diamond nanomechanical resonators that should have superior characteristics (high frequency, high mechanical quality factor, etc.) due to excellent mechanical properties of diamond. These NEMS devices would be of great interest for application in bio-medicine, for example, due to biocompatibility of diamond (carbon-only material).

In Figure 3.20 we show different type of diamond nanostructure that we have fabricated and studied during the last year. These top-down fabricated (using FIB) diamond nanowires have been defined around NV color centers implanted in ultra-pure CVD synthesized diamond (red dots in Fig. 3.20). To the best of our knowledge our work is the first demonstration of NV color center in any optical structure fabricated in diamond. Using these nanowires we have also investigated the influence of unwanted Ga^+ implantation (during FIB milling) on optical properties of our quantum emitters. We found that contrary to predictions Ga^+ does not introduce significant damage to diamond

and does not spoil the properties of color centers. This was a crucial experiment since it demonstrates that FIB milling is a promising route for realization of functional diamond nanostructures.

In conclusion, we believe that our pioneering work on diamond nanostructures will enable faster implementation of diamond as promising nanophotonic and nanomechanic platform for applications ranging from quantum optics to biomedical sensing.

Nanophotonics Devices Based on Semiconductor Nanocrystals

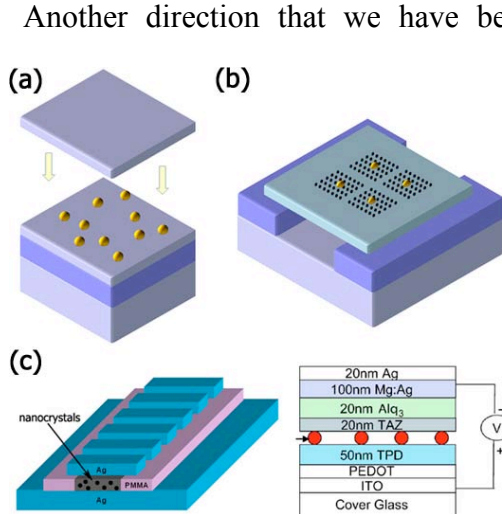


Figure 3.21. (a) NCs are sandwiched between two SiN_x layers and (b) photonic crystal cavities are defined around them. (c) Schematic of electrically injected LED based on metal-insulator-metal plasmonic structure. Electrical injection can be achieved using approach proposed in Reference 7.

Another direction that we have been actively pursuing during the past year is realization of nanoscale optical devices based on semiconductor nanocrystal (NC) quantum dots (QDs). Semiconductor NC QDs (e.g., CdSe) have recently emerged as promising candidates for realization of light sources (LEDs, lasers, single-photon sources), detectors, optical switches and biochemical sensors. Strong quantum confinement of electrons in NCs results in Dirac-like density of electronic states and large optical gain. However, two important shortcomings of NC QDs need to be solved in order to enable their broader application: (i) Long radiative life time ($\tau_{\text{rad}} = 30$ ns at room temperature), and (ii) small modal gain due to small overlap between NC (~5 nm) and optical mode (~500 nm) [4–6]. We are solving these problems by embedding NC QDs into photonic crystal cavities made in silicon nitride films (Fig. 3.21). For example, we have predicted that

NC embedded in photonic crystal cavity will experience increase in radiative recombination rate of at least two orders of magnitude, thus increasing the intensity of light emitted from NC-based devices, minimizing non-radiative recombination and possibly overcoming problems associated with “blinking”.

During the past year we have developed processes for deposition of SiN_x films, using RF sputtering as well as PECVD techniques, on top of NC QDs without introducing any damages to NCs. To the best of our knowledge, there were no previous reports on PECVD deposition of nitride films on top of NCs. We have also developed fabrication techniques for realization of high quality optical devices in SiN_x membranes (e-beam lithography, reactive ion etching, dry-release based on HF-vapor etching, etc.), including optical waveguides and cavities. Presently, we are characterizing these devices. It is important to stress that the experimental work in Lončar group at Harvard started less than a year ago, and all of the above-mentioned fabrication and

characterization efforts have been built-up from ground zero within the last year. This was possible largely due the generous NSEC support.

In parallel with the development of silicon-nitride based nanophotonic platform, we have developed designs for realization of metal-insulator-metal (MIM) electrically injected LEDs based on QDs (Fig. 3.21c). We have also developed analytical techniques to study extraction efficiency of metallic gratings. To the best of our knowledge there were no previous reports that provided analytical expression for the study of extraction of TM polarized light using metallic gratings. We are presently fabricating the MIM structures, and exploring possibility for realization of electrically injected LEDs based on them (Fig. 3c), using approach similar to the one reported in Reference 7. This work will be done in collaboration with M. Bawendi (MIT).

References

- [1] C. Kurtsiefer, S. Mayer, P. Zarda, H. Weinfurter, *PRL* **85**, 290 (2000).
- [2] J. Wrachtrup, F. Jelezko, *J. Physics: Cond. Matt.* **18**, S807 (2006).
- [3] L. Childress, M.V. Gurudev Dutt, J.M. Taylor, A.S. Zibrov, F. Jelezko, J. Wrachtrup, P.R. Hemmer, M.D. Lukin, *Science* **314**, 281 (2006)
- [4] K. T. Shimizu, W. K. Woo, B. R. Fisher, H. J. Eisler, M. G. Bawendi, *PRL* **89**, 117401 (2002).
- [5] B. Lounis, M. Orrit, *Reports on Progress in Physics* **68**, 1129 (2005)
- [6] V. I. Klimov *et al.*, *Science* **290**, 314 (2000).
- [7] H. Huang, A. Dorn, V. Bulovic, M. G. Bawendi, *APL*, **90**, 023110 (2007)